Digest Journal of Nanomaterials and Biostructures Vol. 3, No.3, September 2008, p. 123 - 134

Review Paper

INTERCALATION OF INORGANIC FULLERENE-LIKE (IF) NANOPARTICLES AND NANOTUBES (INT)

F. Kopnov, R. Tenne
Department of Materials and Interfaces, Weizmann Institute, Rehovot 76100, Israel

The recent progress in intercalation of nanotubes and fullerene-like nanoparticles with various metals was reviewed. Nanotubes from layered materials and also those from non layered compounds were discussed. While nanotubes from layered compounds are generically crystalline those of non layered compounds have in most cases a polycrystalline structure. Different intercalation routes were presented and their relative merits and pitfalls were discussed. Furthermore, the changes in the structural and physical properties of the nanoparticles which accompany the intercalation reaction were described. Special attention was paid to the implementation of the nanotubes as a potential electrode material in lithium based batteries.

(Received May 29, 2008; accepted June 2, 2008)

Keywords: Fullerene, Nanoparticle, Nanotube, Intercalation of fullerene-like nanoparticles and nanotubes, Electrode material

1. Introduction

Inorganic nanotubes (INT)/nanowires and fullerene-like particles (IF) represent a rapidly evolving research field. The first inorganic nanotubes and fullerene-like particles were synthesized from layered transitional metal dichalchogenides (TMDS) - 2H-WS_2[1] and 2H-MoS_2[2]. Subsequently it has been shown that various materials with layered structure such as BN[3], V_2O_5[4], NbS_2[5] and many others form closed cage nanostructures. It is worth mentioning that inorganic nanotubes can be produced not only from layered materials. Recent experiments demonstrated that almost perfectly crystalline nanotubes (NT) of 3D compounds with quasi-isotropic structure can be synthesized in a reproducible manner, using removable templates, such as nanowires, etc. Thus faceted GaN nanotubes with hexagonal cross-section were obtained by the reaction of trimethylgallium and ammonia on an ordered array of ZnO nanowires, which served as a template[6]. For an interested reader there are a few extensive reviews such as that by Remskar[7] which is focused on the synthesis and structural aspects of the nanotubes from layered as well as non-layered compounds. Moreover, Rao's *et al.* paper includes an overview of the synthesis of nanobelts, nanowalls and zero-dimensional nanocrystals[8]. Numerous potential applications have been demonstrated for the IF nanoparticles and INT in advanced solid lubrication; mechanical strengthening of nanocomposites and in the longer future for optical and electronic devices. Indeed "ApNano Materials" (www.apnano.com) has recently introduced to the market the first series of solid lubricants based on this nanomaterials technology. These developments make the detailed study of the IF and INT both timely and highly warranted.

The synthesis of the first hollow closed structures from layered materials[1,2] opened up a whole new scientific field in materials science. Some of the chemical and physical properties of these nanomaterials have been studied[9]. Zettl's group[10] for example deposited amorphous $C_9H_{16}Pt$ at one end of BN and carbon NT, thus achieving non-uniform mass-loading geometry. The authors showed that these BN and C nanotubes possessed asymmetric axial thermal conductance properties, with a greater heat flow in the direction of decreasing mass density. Owing to its partially ionic character, the BN NT bandgap of ca. 5.5 eV is almost independent of tube morphology. Therefore, BN NTs are normally insulating. However, flattening deformation or decrease in tube diameter down to 0.4–1 nm or less, or application of a transverse electric field

(Stark effect) diminishes the bandgap, as revealed by theoretical calculations[11]. Lately the experimental evidence in support of the predicted giant Stark effect was reported[12].

Fundamental and applied research on Li-based batteries has drawn extensive attention for more than thirty years[13]. However, further progress in batteries applications are still rather hindered by limitations of the electrode materials. Thus, the ongoing research on novel lithium storage materials is stimulated by the inability of lithium-ion batteries to fully satisfy the energy capacity and power needed for consumer electronics. The interested reader can refer to several excellent reviews on the subject of lithium-based batteries[13, 14]. The progress required in the electrode materials include[14] (i) higher capacity and reversibility for lithium uptake during repeated charge/discharge cycles, (ii) higher lithium diffusivity at high discharge rate, (iii) structural stability over a wider range of lithiation. The emerging new 1D nanostructures, such as nanorods, nanotubes, and nanowires open up new perspectives for Li^+ intercalation applications[15]. It is believed that these new tubular structures can exhibit improved electrochemical performance compared to their polycrystalline counterparts due to their smaller diffusion path and larger surface area. Furthermore, unlike nanorods, nanotubes possess also inner wall surfaces as well as open ends. Therefore, the tubes can operate as effective electrolyte-filled channels having faster transport of lithium ions to the intercalation sites and being able to accommodate large amount of the guest atoms. Moreover, the nanotubes are inherently (meta)stable structures, which in principle, can be reversibly cycled many times.

Among the various lithium-insertion nanomaterials existing today; the current research turns to nanotubes made up from layered structures. The layered nanostructures that have been extensively studied up to date include nanotubes from transitional metal dichalchogenides (TMDS), titanate- $H_2Ti_3O_7$, V_2O_5 and BN. Polycrystalline nanotubes, especially from titania- TiO_2 were investigated as well. The special attention drawn to these structures stems from their unique structure-functionality relationship, as their ability to reversibly intercalate lithium ions. Moreover, these nanomaterials are quite cheap to produce and non toxic compared to various electrode materials, which are currently in use[15,16] . Their large surface area and the accessible space for intercalation in the galleries between the layers make these nanostructures uniquely suitable for such chemical reactions. Additionally, the possibility to intercalate V_2O_5 with Li, Na, and Mg ions opens up possibilities for new applications as electrochromic display devices and large-capacity energy storage batteries[17]. Titania being chemically stable; with strong reducing power and also a biocompatible material has many other potential applications in electrochromic devices[18], photocatalysis[19,20], and dye-sensitized solar cells[21]. Hence, much research has been devoted to the intercalation studies of these nanostructures using different metals and most particularly lithium. The following article reviews the recent developments in intercalation of nanotubes and fullerene-like nanoparticles with different metals. Various intercalation routes will be discussed with special attention paid to the changes in the structural and physical properties of the nanoparticles.

2. Transition-Metal Dichalcogenides Nanotubes

The structural, physical and chemical properties of the layered transition-metal dichalcogenide compounds, MX_2 (M=metal, X=chalcogenide) have been investigated intensively for the past five decades[22]. This is due to their unique structural properties, where the MX_2 layers are bonded by weak van der Waals (vdW) forces through relatively large (several Angstrom) van der Walls gap (Figure 1). The existence of the vdW gap allows facile accommodation of foreign atoms and molecules. In general, the intercalation of foreign atoms/molecules within the vdW gap is promoted by full or partial charge transfer to the host lattice. This charge transfer leads to the modifications of the chemical and physical properties, as the electrical conductivity, magnetic susceptibility and the high sensitivity towards humid atmosphere. Furthermore, the accommodation of the guest atoms in the vdW gap leads to swelling of the lattice parameters, particularly along the *c*-axis.

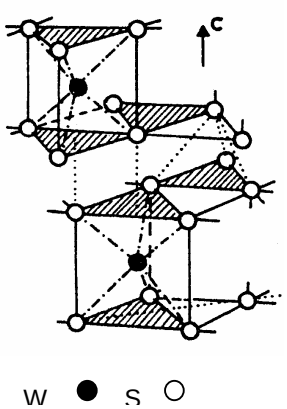

Fig. 1 Crystal structure of 2H-WS_2 (2 stands for two layers in a unit cell, H designates hexagonal symmetry)[22]

It has been possible to interpret many of the changes in the optical and electrical properties of alkali metal intercalated TDMCs in terms of the 'rigid band' model[23]. Within this model the host material band structure is unaltered by the presence of the intercalant except for increased filling of the transition metal *d* band. The justification of this 'rigid band' model stems from the observation that the conduction band, formed from the *d*-band orbitals of the transition metals, is localized at the centre of the MX_2 sandwich. Therefore, with good approximation, relatively small changes occur in the local chemical bonding following intercalation. It is believed that the guest-host charge transfer is the driving force towards intercalation. The rigid band model is thought to hold up to about 10% at. loading of the metal. Thereafter, remarkable changes of band structure of the host take place.

The alkali metals Li, Na, K, Rb, Cs and also simple metals such as Ag and Cu readily enter between the layers of TMDS to form intercalate complexes[23]. Diffraction studies of the intercalated TMDS have revealed a variety of interesting structural changes in the host material. The layer separation in general is found to increase by typically 5-10% for metal intercalates and up to a factor of ten for large organic molecules[24]. Generally the lattice parameter *a* hardly changes upon intercalation, or is observed to change only by up to 1%. A number of experimental methods to intercalate metal atoms in metal dichalcogenide compounds have been developed[23].

Variety of methods have been devised for the synthesis of IF and INT. A few examples for these strategies are pointed out here in brief. The first TMDS closed nanostructures were synthesized by solid-gas reaction at elevated temperatures as high as 840 ^{0}C[23] (Figure 2).

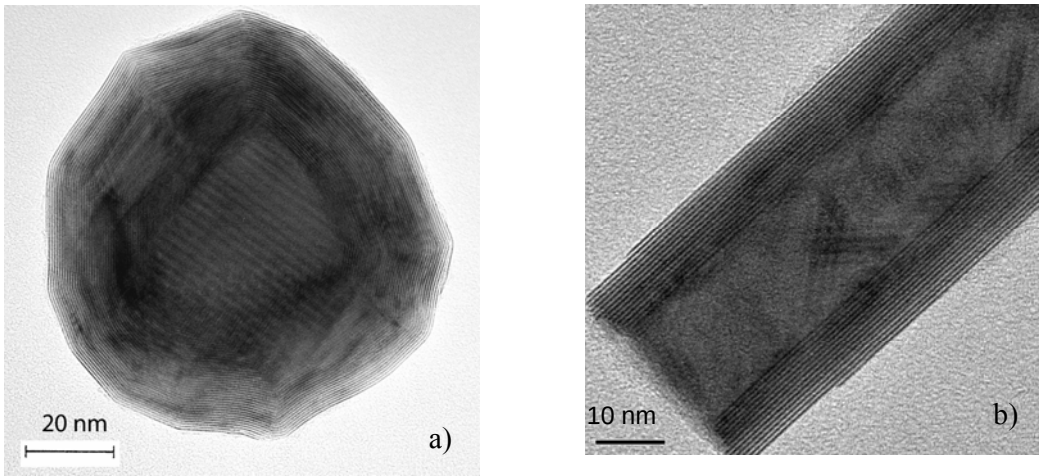

Fig. 2. TEM image of a) fullerene-like WS_2 nanoparticle; b) WS_2 nanotube.

It must be emphasized that practically the synthesis of inorganic closed cage nanostructures and nanotubes is difficult requiring special fine tuning of the reaction conditions in order to avoid the formation of the corresponding bulk layered crystallites. However, recently different synthetic routes have been devised. One of the routes that was proposed for preparation of MS_2 (M=Zr, Hf, W) nanoparticles with fullerene-like structures was by using H_2S and N_2/H_2 gases with auxiliary microwave induced plasma[25] and WO_3 nanoparticles and MS_3 (M=Zr, Hf) phases as precursors. Synthesis of MoS_2 nanotubes using a solid template was also described.[26, 27] This synthetic process is based on a generic deposition strategy, which was suggested by Martin and further improved by Masuda and coworkers[26]. Here, the nanowires/nanotubes are deposited in porous alumina template, which is subsequently dissolves with KOH solution. Recent studies report on the synthesis of WS_2 hollow nanoparticles (IF) via the metal–organic chemical vapor deposition (MOCVD) technique[28] starting from $W(CO)_6$ and elemental sulfur. Furthermore, it is possible to produce IF-Cs_2O nanoparticles by pulsed laser ablation of pure 3R-Cs_2O powder in evacuated quartz ampoules[29]. It is worth mentioning that nanotubes and nanowires of WO_2Cl_2[30] were prepared by a simple process of exfoliation and restacking from the respective crystallites. Intercalation of alkali atoms (Li, Na) of up to two atoms per formula has been demonstrated as well. These are a few examples out of many in this field.

The ability of TDMS to accommodate foreign molecules and atoms opened up vast opportunities for investigating the intercalation of transition metal dichalcogenide nanostructures. Self-assembled $MoS_{2-x}I_y$ (x~/0 and y~/1/3) nanowires bundles can reversibly exchange lithium in non-aqueous electrolytes[31]. Lithium was inserted electrochemically into the $MoS_{2-x}I_y$ nanowires bundles mainly into the interstitial sites. Lithium incorporation took place at negative potentials sufficiently close to that of metallic lithium, making $MoS_{2-x}I_y$ nanowires bundles good candidates for potential negative electrode in Li-ion batteries. Further studies of lithium doped $MoS_{2-x}I_y$ nanowires revealed that these structures possessed a very large, nearly temperature-independent Pauli-like susceptibility[32].

Nanoparticles of MoS_2 and WS_2 were intercalated by exposure to heated alkali metal (potassium and sodium) vapor using a two-zone transport method. The intercalated nanoparticles[33] exhibited a diamagnetic to paramagnetic transition. The *c*-axis of the intercalated WS_2 and MoS_2 inorganic fullerene-like (IF) particles, was expanded up to 18.96 Å for both metals as compared with 12.36 Å for the pristine phase, i.e. interlayer spacing of 9.98 for the metal loaded vs. 6.18 Å for the pure compound. This large expansion was attributed to the hydration of the alkali metals inside the van der Waals gap of the intercalated nanoparticles, which occurred during the X-ray measurements. More recently, intercalation experiments of IF-WS_2 particles with alkali metals[34] (Na, K, Rb), using the same method, were conducted under improved humidity control. The van der Waals gap expansion of the intercalated particles was found to depend on the radius of the alkali atom: the greatest interlayer expansion was obtained for the rubidium intercalation, the least one for the intercalation with sodium atoms. Furthermore, the *a*-axis of the intercalated phase was found to be expanded as well (Fig. 3). The XPS measurements of the Rb intercalated IF-WS_2 powder established that the intercalated material became more electron rich than the pristine one, which led to an upward shift of the Fermi level.

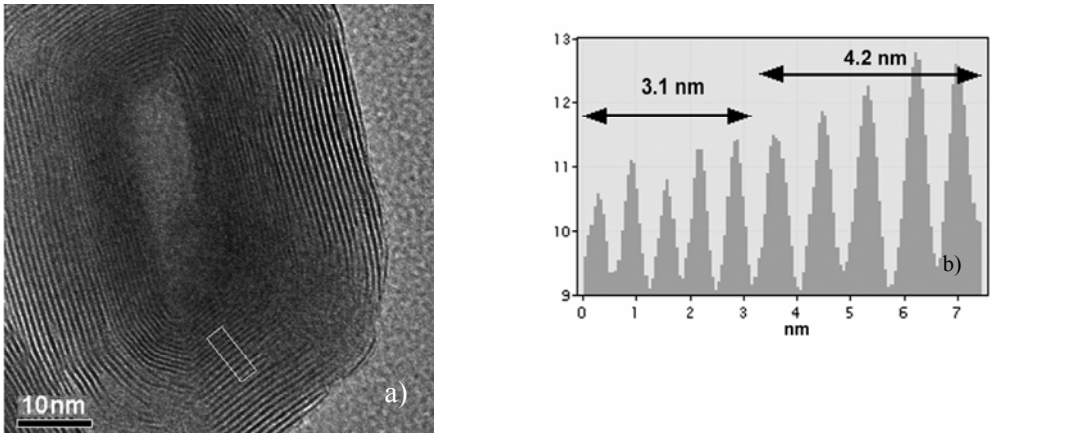

Fig. 3. a) TEM image of a typical rubidium intercalated IF particle, b) the intensity profile of the framed layers at the interface between the pristine (inner) and the intercalated (outer) lattices. The demarcation line between the outermost Rb-intercalated WS_2 layers and the unmodified inner layers is clear.

Furthermore, Li_xTiS_2 nanotubes (x=0.12, 0.52, and 1.0) were prepared by chemical intercalation of the nanotubes using n-BuLi (n-butyl lithium) as the Li source[35]. Only very slight changes were observed in the value of the lattice constant *a*, while the *c* parameter was strongly correlated with the intercalated lithium quantity x. The largest interlayer spacing (6.3 Å) was observed for x=1, which corresponded to *c*-axis expansion of approximately 10.5%. The authors found, that lithium intercalation of TiS_2 nanotubes was as effective as that of the polycrystalline material. It was also shown that TiS_2 nanotubes could undergo reversible electrochemical intercalation-deintercalation process with Mg ions[36]. The atomic ratio between Mg and TiS_2 nanotubes was found to be 0.49:1. The TiS_2 nanotubes electrode demonstrated better electrochemical performance than the polycrystalline one. Particularly, the reversible Mg intercalation of the nanotubes promoted much higher capacity and higher rate of discharge. The authors ascribed this fact to the higher surface area of the tubular structure. However, the report does not provide any information regarding the structural changes of TiS_2 nanotubes upon intercalation.

3. Vanadium Oxide-Alkyl Amine nanotubes

The stereochemistry of vanadium ions in V_2O_5 may be considered to be distorted trigonal bipyramid (five V-O bonds with lengths of 1.58-2.02 Å), distorted tetragonal pyramid or a distorted octahedron (the sixth V-O bond length of 2.79 Å), Figure 4. These weak V-O bonds give rise to the layered structure of vanadium pentoxide crystal. Vanadium pentoxide is of great interest for various technological applications. Supported vanadia films have found vast commercial application as, e.g. oxidation catalyst in the selective oxidation of o-xylene to phthalic anhydride and ammoxidation of alkyl aromatics[37]. The 2D structure of V_2O_5 allows for intercalation of small metal ions such as Li, Na, and Mg in the galleries between the layers. The intercalation process can be accomplished for example, by the electrochemical method[38] or by the vapor phase technique[39,40,]. However, unlike the transitional metal dichalcogenides the influence of the metal intercalants on the electronic properties of V_2O_5 thin films is still not fully understood and is the subject of an ongoing research. Recent XPS studies of either lithium[39,41,42,]or sodium[40] intercalated vanadia thin films showed partial charge transfer from the alkali metal to the V(3d) states. Thus the intercalation process causes partial reduction of vanadium atoms from V^{5+} to V^{4+} and even to V^{3+} as was found in the case of sodium intercalation[40].

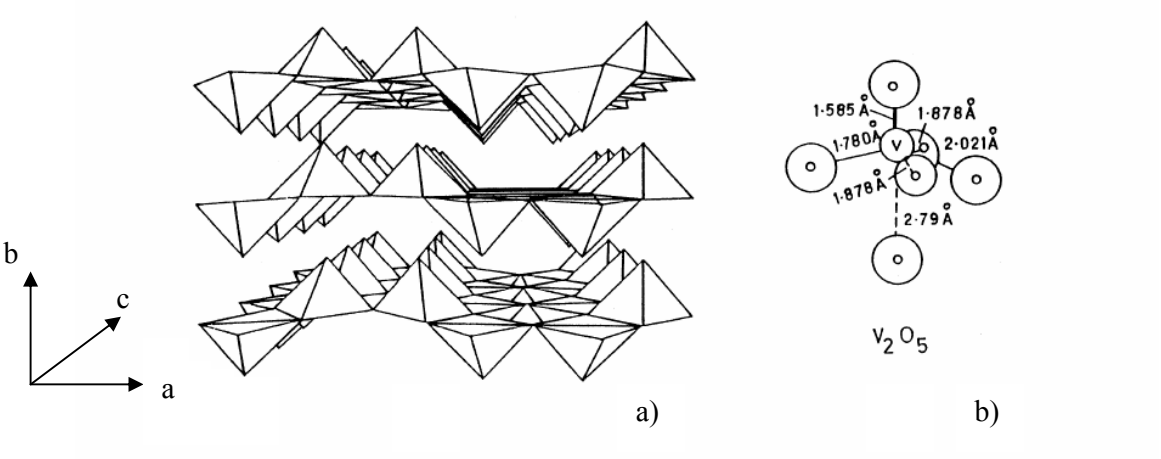

Fig. 4. a) Perspective representation of the lamellar structure of V_2O_5. b) Schematics of the five-fold coordination of vanadium with oxygen atoms in V_2O_5.[43]

The mixed valence vanadium (+4, +5) oxide nanotubes (VO_x NT) (Figure 5) can be easily prepared by low-temperature soft chemical synthesis using alkyl amines as templating agent. The typical synthesis[44,4] involves reaction between vanadium(V) alkoxide precursor primary alkyl amines or α,ω-alkyl diamines which is followed by hydrolysis and hydrothermal reaction. Due to the long alkyl chain template, the interlayer distance becomes 2-4 nm, depending on the length of the alkyl chain and its order. It is possible to replace the expensive vanadium alkoxide with cheaper vanadium(V) oxytrichloride or vanadium(V) pentoxide as a vanadium source[45]. The amine molecules function as a structural directing template and stay between the oxide layers such that the resulted VO_x NT has a scroll-like morphology. Thus electrochemical lithium insertion into scroll-like VO_x nanotubes has been quite extensively studied for the past several years.

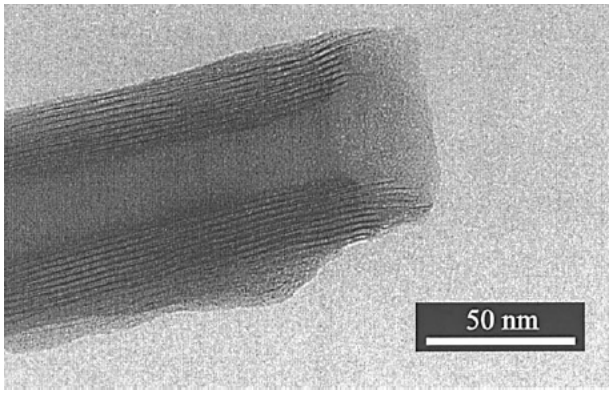

Fig. 5. TEM image of a template-(alkyl amine) containing vanadium oxide nanotube shows the typical open end. [46]

It was shown that the as-synthesized material i.e. with amine template agent had maximum electrical capacities of less than 80 mAh/g[47]. However, alkali, alkali earth and transition ions exchanged VO_x nanotubes showed better electrochemical performance. For example, the Mn

exchanged nanotubes electrochemically intercalated 0.5 lithium per vanadium to a 2 V cutoff, giving a capacity of 140 mAh/g[48]. Moreover, VO_x nanotubes with embedded Na^+, K^+, or Ca^{2+} were obtained[47]. These materials showed charge/discharge reversibly for >100 cycles, giving average capacities of around 150 mAh/g. Nanotubes with embedded amines may have less space for Li^{+1} ions because the amine molecules are bulkier than the metal cations. This could explain the low electrochemical performance of the as prepared VO_x nanoscrolls. There was an attempt to study the mechanism of Li ions electrochemical intercalation inside Ca^{2+} imbedded nanotubes[44]. It was found that there were at least two processes occurring as Li^+ enters the material: a fast decrease of the interlayer distance followed by a slower two-dimensional relaxation of the structure within the VO_x layers.

It is also possible to prepare nanotube arrays of amorphous vanadium pentoxide by template-base electrodepositon[49]. These structures possess high Li^+ intercalation capacity of 300 mAh/g, however, the capacity of the nanotube array decreased and stabilized within 10 cycles at 160 mAh/g.

VO_x nanotubes doped either with lithium or iodine demonstrated ferromagnetic behavior at room temperature[50], which could be useful for spintronics. Moreover, the doping has the effect of shifting the Fermi level from the middle of the energy gap to either the valence (iodine) or the conduction band (lithium), turning this Mott-Hubbard insulator into a good conductor. This behavior was attributed to the removal of the spin frustration in the lattice of the doped nanotubes. Recently VS_2 nanotubes were prepared from VO_x nanotubes by sulfidization with H_2S at 225 ^{0}C. It was shown that VS_2 nanotubes could be electrochemically intercalated with copper up to a composition of $Cu_{0.77}VS_2$[51] .

4. Titanium Oxide and Titanate Nanotubes

Titanium oxide appears in nature in three different forms which, in order of abundance, are rutile, anatase, and brookite. Furthermore, TiO_2 have several artificially synthesized phases[52] as TiO_2 (B), TiO_2 (H), and TiO_2 (R). In all these oxides, titanium is octahedrally coordinated to oxygen atoms. The TiO_6 octahedra share vertices and edges building up thereby a three-dimensional framework of the oxide, and leaving empty sites available for lithium insertion. Electrochemical studies have demonstrated that various modifications of TiO_2 accommodate lithium ions at different ratios. Anatase and TiO_2 (B) can accommodate, according to the different studies, 0.5–1 Li atom per formula[53,54] unit. Lithium insertion into rutile TiO_2 at room temperature is negligible. However, Li can be inserted into rutile TiO_2 without changing the structure at 120 °C up to ≈ 0.25 Li per formula[55]. The ability of anatase and TiO_2(B) polymorphs to accommodate more lithium was attributed to its lower dense structure as compred to that of rutile[48]. Yet, recent studies showed that nanocrystalline rutile could accommodate one lithium atom per formula at room temperature[53]. Lately the intercalation of nanocrystalline brookite was reported[56] as well. It is worth mentioning that there are only a few studies on the influence of the lithium intercalation on the electronic properties of titania. For example, a recent XPS study concluded that electrochemical insertion of lithium ions in nanoporous anatase produced reduced Ti ions (Ti^{3+})[57].

Nanotubular TiO_2 materials, with a typical dimension less than 100 nm, have recently emerged. There are three general approaches to the synthesis of TiO_2 and titanate nanotubes, i.e., chemical (template) synthesis[58], electrochemical approaches[59] (e.g., anodizing Ti foils or films), and the alkaline hydrothermal method[60]. The specific crystal phase of TiO_2 nanotubes and their degree of crystallinity depends on the synthetic routes. The TiO_2 nanotubes produced by templating are usually amorphous or polycrystalline with anatase structure. The crystal structure of electrochemically synthesized polycrystalline TiO_2 nanotubes was reported to correspond to an anatase and rutile mixture[59]. The alkaline hydrothermal synthesis can produce protonated titanate nanotubes, with a crystalline scroll-like layered structure[61]. Subsequent calcination process converts the titanate nanotubes to either polycrystalline TiO_2(B)[62] or anatase[63] ones, and there are even reports on nanotubes consisting of mixed anatase and TiO_2(B) phases[64]. There are several excellent reviews[65,66] which elaborate on the synthesis, morphology and the chemical and physical properties of titania and titanate nanostrucures.

According to the crystal structure of titanate nanotubes, protons occupy the cavities between the layers of TiO_6 octahedra. The open morphology of the nanotubes results in effective ion-exchange properties. For example, protonated trititanate nanotubes $H_{0.7}Ti_{1.825}\square_{0.175}O_4 \cdot H_2O$ (□ vacancy) were intercalated with alkali metal ions (Li^+, Na^+, K^+, Rb^+, Cs^+) by soaking the nanostructures in a metal hydroxide solution[67]. During this process the H_3O^+ ions are expected to be exchanged for alkali metal ions. However, the interlayer distance of ~0.9 nm of the nanotubes remained almost unchanged after the ion exchange reactions. The uptake amount, x mol per formula weight in $A_xH_{0.72-x}Ti_{1.825}\square_{0.175}O_4 \cdot H_2O$ (where A denotes alkali metal cations), for Li^+, Na^+, K^+, Rb^+, Cs^+ was found to be 0.51, 0.53, 0.46, 0.49, 0.44, respectively. The uptake capacity corresponds to 70% consumption of exchangeable protons and a monolayer arrangement of the cations and H_2O molecules in the galleries. The cations, that enter in between the tubular layers pin together adjacent ones, and thus improve the crystallinity of the nanotubes.

Lately, a simple hydrothermal method was developed for incorporating Fe into $H_2Ti_3O_7$ nanotubes[68]. Detailed structural characterization showed that the iron incorporated nanotubes had the same structural framework as the $H_2Ti_3O_7$ nanotubes. The absorption edge of the iron incorporated nanotubes extended notably into the visible region; whereas the pristine $H_2Ti_3O_7$ nanotubes effectively absorb ultraviolet light below 400 nm. Detailed first-principles calculations performed by the authors[69] showed that the introduction of Fe in the interlayer region of $H_2Ti_6O_{14}$ structure brought in delocalized Fe 1D band. This band is formed from overlapping Fe-$3d^2_z$ orbitals along the [010] direction. It is believed that this 1D band effectively reduces the band gap of $H_2Ti_6O_{14}$ and leads to the optical absorption in the visible range.

Recently also, TiO_2(B) nanotubes were investigated as anodes for rechargeable lithium batteries. It was found that they could accommodate up to 338 mAh/g of charge, equivalent to $Li_{1.01}TiO_2$(B) at a potential of ~1.5 V vs Li^+ (1 M)/Li[70]. Furthermore, the Li^+ charging of highly-ordered anatase tubular TiO_2 (Figure 6) was accompanied by a clearly visible electrochromic effect[18]. A reversible color change from very light blue-gray to black, and back, was observed during the cathodic reduction and subsequent oxidation, respectively. The electrochromic effects demonstrated by the amorphous compact oxide and the nanotubes were either very weak or decayed after a few switching cycles. It was hypothesized that the poor reversible color-switching in the case of amorphous oxides was due to trapping of intercalated Li^+ in the non-stoichiometric structure.

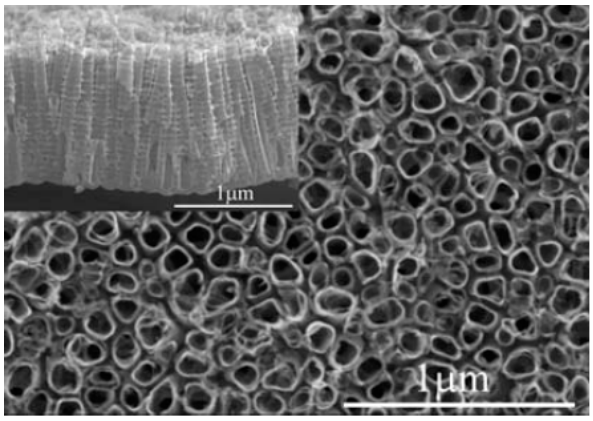

Fig. 6. SEM picture of highly-ordered anatase tubular TiO_2 [18]

5. Nanotubes from other materials

It must be emphasized that besides layered materials there is variety of other inorganic compounds that have been shown to demonstrate good capability for lithium storage. For example, some metal oxides can deliver much higher capacity than commercially available carbon based anode materials in Li-ion batteries. However, the mechanism of the reaction of these oxides with

lithium metal differs from the classic insertion/deinsertion mechanism. A typical case is the SnO_2 electrode. When Li is introduced into SnO_2, first lithium oxide and metal tin are produced and this process is followed by the formation of various Li–Sn alloys[71,72]. In addition, some nanostructured transition metal oxides (MO, M = Co, Ni, Cu or Fe) have also been reported to exhibit high electrochemical capacities for lithium storage; high rate of intercalation/ deintercalation (power) and excellent capacity retention after numerous cycles[73].

Thus much effort is currently invested in the synthesis of nanotubes from non layered compounds. For example, polycrystalline α-Fe_2O_3 nanotubes[74] are prepared by templating method showing almost 5-times better gas-sensing characteristics to alcohol and hydrogen than that of the α-Fe_2O_3 nanoparticles. The difference is ascribed to the higher specific surface area of the nanotubes. Moreover, α-Fe_2O_3 nanotubes can be a promising anode material for Li-ion batteries. Polycrystalline α-Fe_2O_3 nanotubes exhibited a discharge capacity of 1415, 1115, and 890 mAh/g in the 1st, 10th, and 20th cycles, respectively, under a current density of 100 mA/g at 20 °C. After 100 cycles consisting of 100% depth discharge/charge cycles at 100 mA/g, the electrode capacity decreased to 510 mAh/g, which is about 36% of the original value and is still much higher than that of graphite (372 mAh/g). The reversible electrochemical reaction mechanism of Li with Fe_2O_3 nanotubes was proposed to be a displacive redox reaction which can be described as follows:

$$Fe_2O_3 + 6Li^+ + 6e \leftrightarrow 3Li_2O + 2Fe \text{ (positive)},$$
$$6Li \leftrightarrow 6Li^+ + 6e \text{ (negative)},$$
$$Fe_2O_3 + 6Li \leftrightarrow 3Li_2O + 2Fe \text{ (overall)}.$$

Recently, a one-step self-supported topotactic transformation approach for the synthesis of needlelike polycrystalline Co_3O_4 nanotubes[75] was reported. At the early stage of the synthesis, needlelike β-$Co(OH)_2$ nanorods with growth direction along [001] are formed. The surface of the nanoneedles cracks into self-organized small platelets with constant air mediation. Under further air treatment, these loosely organized β-$Co(OH)_2$ nanoplatelets undergo the well-known thermodynamically favorable oxidative reaction: $Co(OH)_2 + O_2 \rightarrow Co_3O_4$, which is promoted by the nanometer-scale size of the platelets and the readily available oxygen. On the other hand, solid materials in the core region of β-$Co(OH)_2$ nanoneedles are continuously evacuated through dissolution and reoxidation/deposition on priorly formed Co_3O_4 at the walls of the precursor nanotubes. Thus, needlelike compact Co_3O_4 nanotubes can be produced with its growth direction along the [111] axis of Co_3O_4. The as-prepared Co_3O_4 nanotubes were tested as a negative electrode in lithium based batteries. These nanotubes showed excellent charge/discharge rate (power) and ultrahigh capacity of about 950 mAh/g with nearly 100% capacity retention for over 30 cycles.

6. Conclusions

The recent progress in intercalation of nanotubes and fullerene-like nanoparticles with various metals was reviewed. Nanotubes from layered materials and also those from non layered compounds were discussed. While nanotubes from layered compounds are generically crystalline those of non layered compounds have in most cases a polycrystalline structure. Different intercalation routes were presented and their relative merits and pitfalls were discussed. Furthermore, the changes in the structural and physical properties of the nanoparticles which accompany the intercalation reaction were described. Special attention was paid to the implementation of the nanotubes as a potential electrode material in lithium based batteries.

References

[1] Y. Q. Liu, C. S. Li, J. H.Yang, Z. Hua, J. M. Li, K. H. Yan, S. H. Zhao, Journal of Materials Science & Technology, **23**, 185 (2007).

[2] V. Lavayen, N. Mirabal, C. O'Dwyer, M. A. Santa Ana, E.Benavente, C. M. Sotomayor Torres, G. Gonzalez, Applied Surface Science **253**, 5185 (2007).
[3] N. G. Chopra, R. J. Luyken, K. Cherrey, V. H. Crespi, M. L. Cohen, S. G. Louie, A. Zettl, Science **269**, 966, (1995).
[4] H. J. Muhr, F. Krumeich, U. P. Schonholzer, F. Bieri, M. Niederberger, L. J. Gauckler, R. Nesper, Advanced Materials **12**, 231 (2000).
[5] Y. Q. Zhu, W. K.Hsu, H. W. Kroto, D. R. M. Walton, Journal of Physical Chemistry B **106**, 7623, (2002).
[6] J. Goldberger, R. R. He, Y. F. Zhang, S. W. Lee, H. Q.Yan, H. J. Choi, P. D. Yang, Nature, **422**, 599 (2003).
[7] M. Remskar, Advanced Materials **16**, 1497 (2004).
[8] C. N. R. Rao, S. R. C. Vivekchand, K. Biswasa, A. Govindaraja, Dalton Transactions 3728, (2007).
[9] R. Tenne, Nature Nanotechnology, **1**, 103 (2006).
[10] C. W. Chang, D. Okawa, A. Majumdar, A. Zettl, Science **314**, 1121 (2006).
[11] K. H. Khoo, M. S. C. Mazzoni, S. G. Louie, Physical Review B, **69**, 201401, (2004)
[12] M. Ishigami, J. D.Sau, S. Aloni, M. L. Cohen, A. Zettl, Physical Review Letters **94**, 056804 (2005).
[13] M. Winter, J. O. Besenhard, M. E. Spahr, P. Novák, Advanced Materials **10**, 72, (1998).
[14] J. M.Tarascon, M. Armand, Nature **414**, 359, (2001).
[15] Q. Wang, Z. Wen, J. Li, Inorganic Chemistry, **45**, 6944 (2006).
[16] Y. Wang, K.Takahashi, K. Lee, G. Z. Cao, Advanced Functional Materials **16**, 1133 (2006).
[17] A. Talledo, C. G. Granqvist, Journal of Applied Physics, **77**, 4655 (1995).
[18] R.Hahn, A. Ghicov, H. Tsuchiya, J. M. Macak, A. G. Munoz, P. Schmuki, Physica Status Solidi (a), **204**, 1281 (2007).
[19] A. Wold, Chemistry of Materials **5**, 280. (1993).
[20] D. Dumitriu, A. R. Bally, C. Ballif, P.Hones, P. E. Schmid, R.Sanjinés, F. Lévy, V. I. Pârvulescu, Applied Catalysis B, **25**, 83, (2000).
[21] K.Hara, Y. Dan-oh, C. Kasada, Y. Ohga, A. Shinpo, S. Suga, K.Sayama, H. Arakawa, Langmuir, **20**, 4205 (2004).
[22] J. A. Wilson, A. D. Yoffe, Advances in Physics **18**, 193 (1969).
[23] R. H. Friend, A. D. Yoffe, Advances in Physics **36**, 1, (1987).
[24] A. P. Legrand, S. Flandrois, North Atlantic Treaty Organization. Scientific Affairs Division. Chemical physics of intercalation; Plenum: New York, 1987.
[25] D. J.Brooks, R. E. Douthwaite, R. Brydson, C. Calvert, M. G. Measures, A. Watson, Nanotechnology **17**, 1245 (2006).
[26] H. Masuda, K. Fukuda, Science, **268**, 1466 (1995).
[27] C. M. Zelenski, P. K. Dorhout, Journal of the American Chemical Society **120**, 734 (1998).
[28] M. N. Tahir, N. Zink, M. Eberhardt, H. A. Therese, S. Faiss, A. Janshoff, U. Kolb, P. Theato, W. Tremel, Small, **3**, 829 (2007).
[29] A.Albu-Yaron, T. Arad, M. Levy, R. Popovitz-Biro, R. Tenne, J. M. Gordon, D.Feuermann, E. A. Katz, M. Jansen, C. Mühle Advanced Materials, **18**, 3199 (2006).
[30] A. R. Armstrong, J. Canales, P. G. Bruce, Angewandte Chemie International Edition **43**, 4899, (2004).
[31] R. Dominko, M.Gaberscek, D. Arcon, A.Mrzel, M.Remskar, D.Mihailovic, S. Pejovnik, J. Jamnik, Electrochimica Acta **48**, 3079, (2003).
[32] Z. Jaglicic, A. Jeromen, Z. Trontelj, D. Mihailovic, D. Arcon, M. Remskar, A. Mrzel, R. Dominko, M. Gaberscek, J. M. Martinez-Agudo, C. J. Gomez-Garcia, E. Coronado, Polyhedron, **22**, 2293, (2003)Magnetic properties of MoS_2 nanotubes doped with lithium.
[33] A. Zak, Y. Feldman, V. Lyakhovitskaya, G. Leitus, R. Popovitz-Biro, E. Wachtel, H. Cohen, S. Reich, R. Tenne, Journal of the American Chemical Society **124**, 4747 (2002).
[34] F. Kopnov, Y. F eldman, R. Popovitz-Biro, A. Vilan, H. Cohen, A. Zak, R. Tenne, Chemistry of Materials (to be published). Intercalation of alkali metal in WS_2 nanoparticles, revisited.
[35] J. Chen, Z. L. Tho, S. L. Li, Angewandte Chemie-International Edition **42**, 2147 (2003).

[36] Z.-L. Tao, L.-N. Xu, X.-L. Gou, J. Chen, H.-T.Yuan, Chemical Communications, 2080 (2004).
[37] I. E. Wachs, B. M. Weckhuysen, Applied Catalysis (a), **157**, 67 (1997).
[38] V. Shklover, T. Haibach, F. Ried, R. Nesper, P. Novak, Journal of Solid State Chemistry, **123**, 317 (1996).
[39] F. Donsanti, K.Kostourou, F. Decker, N. Ibris, A. M. Salvi, M.Liberatore, A. Thissen, W. Jaegerman, D. Lincot, Surface and Interface Analysis **38**,815 (2006).
[40] Q.-H. Wu, A. Thien, W. Jaegermann, Solid State Ionics **167**, 155, (2004).
[41] J. Swiatowska-Mrowiecka, F. Martin, V. Maurice, S. Zanna, L. Klein, J. Castle, P. Marcus, Electrochimica Acta **53**, 4257 (2008).
[42] J. Swiatowska-Mrowiecka, V. Maurice, S. Zanna, L. Klein, Marcus, P. Electrochimica Acta, **52**, 5644, (2007).
[43] C. V. Ramana, O. M. Hussain, B. S. Naidu, C. Julien, M. Balkanski, Materials Science and Engineering B, **52**, 32 (1998).
[44] S. Nordlinder, L. Nyholm, T. Gustafsson, K. Edstrom, Chemistry of Materials **18,** 495 (2006).
[45] M. Niederberger, H. J.Muhr, F. Krumeich, F. Bieri, D. Gunther, R. Nesper, Chemistry of Materials **12**, 1995 (2000).
[46] M. E. Spahr, P. Stoschitzki-Bitterli, R. Nesper, O. Haas, P. Novák Journal of the Electrochemical Society **146**, 2780 (1999).
[47] N. Sara, L. Jan, G. Torbjorn, E. Kristina, ECS, Journal of the Electrochemical Society **150**, E280 (2003).
[48] A. Dobley, K.Ngala, S. Yang, P. Y. Zavalij, M. S. Whittingham, Chemistry of Materials **13**, 4382 (2001).
[49] Y. Wang, K. Takahashi, H. Shang, G. Cao, Journal of Physical chemistry B, **109**, 3085 (2005).
[50] L. Krusin-Elbaum, D. M. Newns, H. Zeng, V. Derycke, J. Z. Sun, R. Sandstrom, Nature **431**, 672 (2004).
[51] H. A. Therese, F. Rocker, A. Reiber, J. Li, M. Stepputat, G. Glasser, U. Kolb, W. Tremel, Angewandte Chemie International Edition **44**, 262 , (2005).
[52] A. Kuhn, R. Amandi, F. García-Alvarado, Journal of Power Sources **92**, 221 (2001).
[53] M. A. Reddy, M. S. Kishore, V. Pralong, V.Caignaert, U. V. Varadaraju, B. Raveau, Electrochemistry Communications **8**, 1299 (2006).
[54] M. Zukalova, M. Kalbac, L. Kavan, I. Exnar, M. Graetzel, Chemistry of Materials **17***,* 1248, (2005).
[55] K.Ladislav, F. Dina, K. Petr, Electrochemical and Solid-State Letters **146,** 1375 (1999).
[56] M. A. Reddy, M. S. Kishore, V. Pralong, U. V.Varadaraju, B. Raveau, ECS, 2007; Vol. 10. Reddy, M. A.; Kishore, M. S.; Pralong, V.; Varadaraju, U. V.; Raveau B., Electrochemical and Solid-State Letters **10**, A29 (2007).
[57] S. Södergren, H. Siegbahn, H. Rensmo, H. Lindstro1m, A. Hagfeldt, S. Lindquist, Journal of Physical Chemistry B, **101**, 3087 (1997).
[58] S. M. Liu, L. M. Gan, L. H. Liu, W. D. Zhang, H. C. Zeng, Chemistry of Materials **14**, 1391 (2002).
[59] E.Balaur, J. M. Macak, L. Taveira, P. Schmuki, Electrochemistry Communications **7**, 1066, (2005).
[60] T. Kasuga, M. Hiramatsu, A. Hoson, T. Sekino, K. Niihara, Langmuir **14**, 3160 (1998).
[61] Q. Chen, W. Z. Zhou, G. H. Du, L. M. Peng, Advanced Materials **14**, 1208, (2002)
[62] E. Morgado, P. M. Jardim, B. A. Marinkovic, F. C. Rizzo, M. A. S. De Abreu, J. L. Zotin, A. S. Araujo, Nanotechnology **18**, 495710 (2007).
[63] D. Wang, F. Zhou, Y. Liu, W. Liu, Materials Letters **62**, 1819, (2008).
[64] L. P. An, X. P. Gao, G. R. Li, T. Y. Yan, H. Y. Zhu, P. W. Shen, Electrochimica Acta, **53**, 4573, (2008).
[65] D. V. Bavykin, J. M. Friedrich, F. C. Walsh, Advanced Materials, **18**, 2807 (2006).
[66] H.-H. Ou, S.-L. Lo, Separation and Purification Technology **58**, 179, (2007).
[67] R. Z. Ma, T. Sasaki, Y. Bando, Chemical Communications, 948, (2005).
[68] X. Ding, X. G. Xu, Q. Chen, L. M. Peng, Nanotechnology **17**, 5423, (2006).

[69] X. G. Xu, X. Ding, Q.Chen, L. M. Peng, Physical Review B, **73**, 165403, (2006)
[70] G. Armstrong, A. R. Armstrong, J. Canales, P. G. Bruce, Electrochemical and Solid-State Letters **9**, A139 (2006).
[71] Ian A. Courtney, J. R. Dahn, Journal of Electrochemical Society **144**, 2045 (1997).
[72] Z. Ying, Q. Wan, H. Cao, Z. T. Song, S. L. Feng, Applied Physics Letters **87**, 113108 (2005).
[73] F. Y. Cheng, J. Chen, Journal of Materials Research **21**, 2744, (2006).
[74] J. Chen, L. Xu, W. Li, X. Gou, Advanced Maretials, **17**, 582 (2005).
[75] X. W. Lou, D. Deng, J. Y. Lee, J. Feng, L. A. Archer, Advanced Materials, **20**, 258 (2008).